Approaches to Modeling Coupled Flow and Reaction in a 2-D Cementation Experiment

B. COCHEPIN[1,*], L. TROTIGNON[1], O. BILDSTEIN[1], C.I. STEEFEL[2], V. LAGNEAU[3], J. VAN DER LEE[3]

[1] *Direction de l'Energie Nucléaire, CEA Cadarache, Bât. 307, 13 108 Saint Paul lez Durance, France*

[2] *Earth Sciences Division, Lawrence Berkeley National Laboratory, 1 Cyclotron Road, Mail Stop 90-1116, Berkeley, CA 94720, USA*

[3] *Centre de Géosciences-Ecole des Mines de Paris, 77305 Fontainebleau, France*

KEYWORDS: Reactive transport, hydrodynamics, porosity clogging, numerical benchmarking, mineral surface area, simulation, coupled processes, Crunch, Hytec.

[*] Corresponding Author.
E-mail address : benoit.cochepin@cea.fr (B. Cochepin)

ABSTRACT:

Porosity evolution at reactive interfaces is a key process that governs the evolution and performances of many engineered systems that have important applications in earth and environmental sciences. This is the case, for example, at the interface between cement structures and clays in deep geological nuclear waste disposals. Although in a different transport regime, similar questions arise for permeable reactive barriers used for biogeochemical remediation in surface environments.

The COMEDIE project aims at investigating the coupling between transport, hydrodynamics and chemistry when significant variations of porosity occur. The present work focuses on a numerical benchmark used as a design exercise for the future COMEDIE-2D experiment. The use of reactive transport simulation tools like Hytec and Crunch provides predictions of the physico-chemical evolutions that are expected during the future experiments in laboratory. Focus is given in this paper on the evolution during the simulated experiment of precipitate, permeability and porosity fields.

A first case is considered in which the porosity is constant. Results obtained with Crunch and Hytec are in relatively good agreement. Differences are attributable to the models of reactive surface area taken into account for dissolution/precipitation processes. Crunch and Hytec simulations taking into account porosity variations are then presented and compared. Results given by the two codes are in qualitative agreement, with differences attributable in part to the models of reactive surface area for dissolution/precipitation processes. As a consequence, the localization of secondary precipitates predicted by Crunch leads to lower local porosities than for predictions obtained by Hytec and thus to a stronger coupling between flow and chemistry. This benchmark highlights the importance of the surface area model employed to describe systems in which strong porosity variations occur as a result of

dissolution/precipitation. The simulation of highly non-linear reactive transport systems is also shown to be partly dependent on specific numerical approaches.

1. Introduction

Porosity evolution is a key process that governs the evolution and efficiency of many engineered systems that have important applications in earth and environmental sciences. This is the case, for example, at the interface between waste packages structures (cement, carbon steel) and clays in deep geological nuclear waste disposals [1, 2]. Similar questions arise, although under different transport conditions, for permeable reactive barriers used for biogeochemical remediation in surface environments [3, 4]. Other examples of porosity clogging with a strong reduction of permeability resulting in unfavorable conditions can be found in oil reservoir engineering [5], in hydrothermal systems [4, 6], in soil science with "bioclogging" in landfill leachate treatment operations and constructed wetlands for waste water disposal [7, 8]. This phenomenon does not necessarily produce adverse conditions, for instance in the case where porosity decrease does not directly affect the permeability or even induces a decrease of the efficiency of initial preferential pathways by increasing residence time [9]. It may also improve the confinement properties where circulation of fluids is undesirable by building a barrier to aggressive agents, thus reducing the reactivity between regions in a system.

Reactive transport simulation tools, used to simulate the geochemical evolution of porous media, frequently integrate a description of porosity/permeability variations due to mineralogical transformations coupled to flow field evolution [10-12]. However, because of the complexity and non-linearity of processes involved, this does not guarantee that equivalent (or even comparable) predictions will be obtained with these different modelling

tools. In order to improve our confidence in numerical predictions and to identify critical features of the models involved, it is necessary to develop comparative simulations of dedicated experiments or systems.

Such an experiment was proposed and performed in a 1-D geometry by Lagneau [13]. A 2-D version of the same system, named COMEDIE-2D, was explored by Trotignon et al. [14]. The present paper is a further step towards such a 2-D experiment which will contribute to the validation of reactive transport simulation tools. Two codes, Hytec [10] and Crunch [15], using different simulation approaches and algorithms were used to simulate the same two-dimensional porous medium in which strong porosity/permeability variations occur due to dissolution/precipitation reactions. In this paper, the characteristics of the system will be first introduced. The two simulation tools will then be presented with emphasis given to their respective porosity/permeability models. Finally, after a description of the simulation results, elements will be proposed to explain the observed differences.

2. Definition of the experimental set-up

A 2-D cementation experiment in a porous medium was previously dimensioned with Hytec [14]. The selected experimental design involves the successive precipitation and perforation of a clogging obstacle made with calcium oxalate. The constraints imposed to design this experiment are:

- The desired characteristic length of the chamber is ~10 cm so that construction and instrumentation of the future experiment at the laboratory remains feasible;
- The duration of this experiment is about 3 months.

Note that the size of the experimental system has been modified since the original design presentation in [14] (140 mm instead of 280 mm) in order to shorten the total experiment duration.

Reactants (oxalate ions) are injected with a constant flux in a porous medium, which locally contains the mineral portlandite. The chemical reaction between the inlet solution and portlandite ($Ca(OH)_2$) leads to the precipitation of calcium oxalate ($CaC_2O_4.H_2O$) following the reaction:

$$C_2O_4^{2-} + Ca(OH)_2 + H_2O \Rightarrow CaC_2O_4 \cdot H_2O + 2OH^- \quad (1)$$

This transformation induces a volume decrease of 33 mL per mol of reacted portlandite, leading to clogging of the porous medium. The experimental chamber is a square box (140x140 mm²) (Figure 1) with two inlets (20 mm) and one outlet (40 mm) for fluid circulations. The porous medium is homogeneous and composed of quartz sand (considered as a chemically inert phase in the simulations), except for a rectangular zone (20 mm of width) located in the middle of the box which contains also portlandite grains. The main properties of this chamber are reported in Table 1.

The initial effective properties of each zone were evaluated with the hypothesis that quartz is composed of regular spherical grains (with a diameter of about 100 µm) and of very small portlandite grains (with a diameter around 1 µm) dispersed in the interstices of the quartz grains. The fluid inlets 1 and 2 are supplied respectively with dilute solutions of sodium chloride and sodium oxalate with physical and chemical properties reported in Table 2. A constant flux of solutes is imposed as boundary condition at the inlets, whereas the outlet boundary condition is a constant head.

The activity of H_2O was fixed at 1 in all simulations. The oxalate ion $C_2O_4^{2-}$ was introduced as a new basis species in the thermodynamic database, implying that the system is not in overall redox equilibrium. Several aqueous complexes between the oxalate ion and calcium, sodium and the proton were also introduced using the thermodynamic constants of the Harwell Hatches database [16]. The equilibrium constant for the Ca-oxalate precipitate was calculated from data given in Lide [17]. The chemical species considered in the simulation were restricted and equilibrium constants for the considered reactions are listed in Table 3.

3. Constitutive equations and fundamental differences between numerical tools

3.1. Fundamental equations

The governing equations of the problem are obtained in the framework of the physicochemistry of nondeformable porous media. Since all physical quantities relate to a representative elementary volume (REV) of porous medium, the mass balance of species and transport equations are represented by means of partial differential operators using position, time, concentration, porosity, permeability, etc as continuous variables. The different chemical concentration fields are treated using the classical approach of chemical components [18-21]: all the m species X_j with concentration c_j in the system can be written using a minimum basis of n components (represented by basis species C_i, $i = 1, \ldots, n$) with total concentration c_i^{tot} ($i = 1, \ldots, n < m$), using the stoichiometric coefficients α_{ij}, so that:

$$\forall \mathrm{j} \in \left[\ 1,..., \mathrm{m}\right] \quad , \quad \sum_{i=1}^{n} \alpha_{ij} C_i \leftrightarrow X_j \qquad (1)$$

The chemical system is modeled by a system of algebraic (thermodynamic equilibrium) and/or partial derivative (kinetic control) equations. The transport equation of a chemical component may be written as:

$$\frac{\partial(\omega X_j)}{\partial t} = \mathrm{div}\left(D^* \overrightarrow{\mathrm{grad}}\, X_j - X_j \vec{U}\right) + R(X_1, ..., X_m) \qquad (2)$$

where ω is the local porosity, $\vec{U}$ the Darcy velocity and D^* the dispersion-diffusion tensor and R denotes the source/sink term caused by all chemical reactions affecting the chemical component. In this equation, the concentrations are given in mole per volume of solution. In the present case, diffusion and dispersion are assumed isotropic and D^* reduces to a scalar form, $D^* = \alpha\left|\vec{U}\right| + D$ ($m^2.s^{-1}$), where D is the effective diffusion coefficient assumed to take the same value for all solutes and α (m) is the dispersivity of the porous medium. The choice of isotropic dispersion is imposed by the current version of Hytec which allows only isotropic dispersion tensor. All reactions between aqueous species are considered at equilibrium.

Several of the physical laws governing chemistry and transport are not identically described in the reactive transport codes Crunch [1] and Hytec [10] used in this work. Table 4 and Table 5 present the most significant disparities between Hytec and Crunch, which could be sources of discrepancies in the benchmark calculations.

Two phenomenological laws are assumed to relate porosity, permeability and the diffusion coefficient of solutes in the porous medium. In the case of Hytec, the intrinsic permeability k_s at saturation (expressed in unit of square distance), is related to porosity, with a normalized form of the Kozeny-Carman relationship adapted by Lagneau [13]:

$$k_S = k_0 \left(\omega / \omega_0\right)^3 \left[(1-\omega_0)/(1-\omega)\right]^2 \qquad (3)$$

And the dispersion coefficient is related to porosity and saturation as follows:

$$D^* = D_e(\omega)\frac{\theta}{\omega} + \alpha|\mathrm{U}| \tag{4}$$

Where α is the dispersivity, θ is the saturation and D_e is the effective diffusion coefficient in saturated conditions. D_e is a function of ω according to Archie's modified law:

$$D_e(\omega) = D_e(\omega_0)\left(\frac{\omega - \omega_c}{\omega_0 - \omega_c}\right)^a \tag{5}$$

Where ω_0 is the initial porosity, ω_c is a critical minimal porosity below which diffusive transfer is negligible and a is Archie's empirical coefficient. In this study, the critical porosity in Hytec (ω_c) is set to 0 in order to obtain expressions that can match the diffusion law used in Crunch. Equations (3) and (5) are semi-empirical and greatly simplified descriptions of processes that are very complex at the microscopic scale. However, in many cases they describe the expected behavior at the macroscopic scale [22].

The dependence of dispersivity α on porosity and permeability changes is expected to be small [23], although dispersion (i.e. $\alpha\left|\vec{U}\right|$) should decrease progressively with increasing cementation of the porous medium as the Darcy velocity of the fluid drops. The flow velocity evolution is assumed to be governed by Darcy's law, written here using the hydraulic head h:

$$\vec{U} = -K_s\,\overrightarrow{\mathrm{grad}}(h) \tag{6}$$

and by the continuity equation:

$$\mathrm{div}(\rho\vec{u}) + \frac{\partial(\rho\omega)}{\partial t} = 0 \tag{7}$$

where $\vec{u}$ is the fluid pore velocity (related to the Darcy velocity by $\vec{U} = \omega\vec{u}$), ρ is the fluid density and K_s is the hydraulic conductivity at saturation (expressed in unit of distance per

unit of time), also called dynamic permeability. The dynamic permeability K_s is directly related to the intrinsic permeability k_s by using the density and dynamic viscosity of the fluid. Under several assumptions (compressibility, etc…), the combination of (6) and (7) leads to the diffusivity equation, i.e.:

$$\mathrm{div}\left(K_s \, \overrightarrow{\mathrm{grad}}(h)\right) = S_s \frac{\partial h}{\partial t} + q \qquad (8)$$

where S_s (m^{-1}) is the storage coefficient and q is a source term accounting here for porosity variations due to chemical reactions.

The reference simulations conducted with Hytec were done with the assumption of local chemical equilibrium. This is equivalent to considering infinite reacting surface areas for minerals, whatever the local porosity. Hytec is also able to work in kinetic mode with different possibilities for defining reaction rates and reactive surface areas, as summarized in Table 5. Several runs were conducted in kinetic mode with Hytec in order to evaluate the effects of finite reactions rates.

In the case of Crunch [15], the intrinsic permeability k_s follows the relation:

$$k_s = k_0 \left(\omega / \omega_0 \right)^3 \qquad (9)$$

The relation between permeability and porosity described in equation (9) is not strictly equivalent to the relation used in Hytec (equation (3)); the difference of permeability values is negligible for porosity values near ω_0, but the difference can reach forty percent at the maximum of the clogging phase. This difference will have to be considered in the interpretation of eventual discrepancies between predictions.

The combined dispersion-diffusion tensor is defined in Crunch as the sum of the mechanical or kinematic dispersion coefficient D' and the molecular diffusion coefficient, D_0, in water divided by the formation factor, F:

$$\mathrm{D} = \mathrm{D}' + \frac{D_0}{F} \tag{10}$$

Usually, F is defined as the ratio of the resistivity of the saturated porous medium over the resistivity of the pore solution alone. F may also be defined in numerous ways, but here a definition based on Archie's Law is used which gives the formation factor the following form:

$$F = \omega^{-m} \tag{11}$$

where m is the "cementation exponent". It is necessary that a equals m (see Table 1, first row) in order to obtain equivalent expressions in Crunch and Hytec. In addition, the following relationship has to be respected between D_0 (Crunch) and D_e (Hytec):

$$D_0\,(Crunch) = \frac{D_e\left(\omega_0\right)}{\omega_0^a}\,(Hytec) \tag{12}$$

In these conditions, variations of the diffusion coefficient with porosity will be identical in Hytec and Crunch simulations. In this presentation of the benchmark, coefficients a and m were arbitrarily set to 1: this corresponds to a porous medium with no tortuosity. Actually, values of a (resp. m) greater than 1 would be required to model properly the zone containing portlandite in which porosity has a more complex structure than in the other zones filled only with quartz sand.

Dissolution/precipitation reactions are modeled (necessarily in Crunch and optionally in Hytec) by using kinetic rate laws [15]. The constraint of local equilibrium may be approached by using high reaction rates. Several possibilities are available in Crunch in order to describe reactive surface area, 'bulk surface area' (m^2 per m^3 of porous medium) or 'specific surface area' (m^2 per gram of solid), whereas Hytec needs a 'bulk surface area' in units of m^2 per m^3

of solution. In addition, reactive surface areas of minerals are updated in Crunch differently depending on whether the minerals are primary or secondary phases. In particular, reactive surface area of secondary minerals not initially present that redissolve is set arbitrarily to 1000 m^2/m^3 in Crunch, whereas Hytec needs the definition of some initial nuclei (set in this study to 1 m^2/m^3 of solution). These assumptions lead to asymmetrical dissolution/precipitation laws [15] summarized in Table 5.

Note that Crunch surface area models are designed so that all reactive surface areas tend to 0 when porosity tends to 0 thanks to the $(\omega/\omega_0)^{2/3}$ term (Table 5). This is not always the case in Hytec. For example, when the reactive surface area is specified as a specific surface area, because the multiplying $(\omega/\omega_0)^{2/3}$ term is not included in this model, it doesn't ensure that the surface area tends to 0 when porosity tends to 0. All these specific features and approaches make very difficult the exact reproduction of the same formulation with both codes.

The update of flow in Crunch (equation (8)) is done by taking into account only the source term due to porosity variations. The effect of storage is neglected.

Finally, it must be noticed that the activity correction model used in Hytec is the truncated Davies formula, while Crunch uses the Debye-Hückel activity correction model [24].

3.2. Numerical schemes

The operator splitting method is, among the several numerical methods available for the integration of reactive transport models, a classical approach proposed by Yeh and Tripathi [19]. Several variants of this approach, in which the operators describing respectively transport and chemical reactions are solved separately, exist [21]. Transport and chemistry are solved one after the other within a single time step. In Hytec, the operator splitting method is the "sequential iterative approach" described by De Windt et al. [25], in which, at each time

step, iterations between the transport and chemistry operators are performed until a definite convergence criterion is achieved. The chemical solver for Hytec is the geochemical module Chess [10], and the transport solver for Hytec is R2D2, which uses a finite volume scheme [26]. In Crunch, the operator splitting approach OS3D [27] is a non iterative algorithm, in which the time step magnitude is constrained by a criterion that ensures that the error due to operator splitting remains sufficiently small. Yeh and Tripathi [19] cite the major advantage of the operator splitting or sequential iteration approach as the lower memory requirements of these methods compared to the global implicit and the greater speed at which a single time step can be completed. In addition, probably the most significant advantage of the time splitting approach is the ability to use specific algorithms for high Peclet number transport (i.e., advection dominating over dispersion and molecular diffusion). OS3D uses a third order accurate total variation diminishing or TVD method proposed by Gupta et al. [28]. The TVD algorithm results in significantly less numerical dispersion than the upwind scheme used in the global implicit approach (GIMRT [29, 30], for example).

Both simulation tools update the local permeability after each time step of the calculation. This explicit scheme requires that the time step remains sufficiently small in case of strong couplings between flow and chemical reactions. The sensitivity of results to time step magnitude was therefore explored by allowing in different runs the maximum time step values from ~1300 s to ~40 s. The mesh used is composed of squares with identical sizes (3.3 mm of edge size) over the entire extent of the chamber.

3.3. Kinetics vs local equilibrium issues

As quoted in §3.1, an important difference between Crunch and Hytec is related to the description of dissolution/precipitation reactions. In Crunch, the only possibility is to use an explicit kinetic rate law to describe mass transfer between solution and mineral phases. In

Hytec, it is possible to describe those mass transfers by kinetic rate laws, or to use, in the case of fast reactions, the hypothesis of local equilibrium between minerals and the solution (see Table 5). Under this assumption, mass transfer between mineral phases and the solution are calculated so that local thermodynamic equilibrium is achieved. In the present study, Hytec simulations presented in the following section were conducted with the assumption of local equilibrium (assumption taken in the previous dimensioning work of the COMEDIE-2D experiment [14]). Some results of Hytec with the kinetic hypothesis will only be presented in the discussion part. High rate constants were assumed in Crunch experiments to cause fast mass transfer, thus approaching the local equilibrium condition (see Table 5).

Characteristic time scales for transport and chemistry processes can be evaluated as follows. The characteristic length L is the size of discretization cells, i.e. 3.3 10^{-3} m. The order of magnitude of the Darcy fluid velocity $\vec{U}$ is in the range of 10^{-8}-10^{-6} m.s^{-1}. The timescale of advective transport through an individual cell is thus:

$$\Delta t_1 = \frac{L}{U} \approx 3.3\ 10^{3} - 3.3\ 10^{5}\, s \qquad (13)$$

The dispersion length is $\alpha = 2\ 10^{-2}$ m and the molecular diffusion coefficient is $D = 10^{-9}$ m^2.s^{-1}. The timescale of diffusive-dispersive transport through an individual cell is thus:

$$\Delta t_2 = \frac{L^2}{(\alpha U + D)} \approx 5\ 10^{2} - 10^{4}\, s \qquad (14)$$

So, these transport parameters result in mixed diffusive and advective control (Peclet number, $P_e = 3\ 10^{-2} - 3$ and Courant number, $N_c = 10^{-3} - 10^{2}$).

Kinetic rates k_{rate} were set to 10^{-5} mol.m^{-2}.s^{-1}, the bulk surface area A_{bulk} to 10^3 m$^2_{solid}$.m$^{-3}_{porous\ medium}$ for both portlandite and Ca-oxalate in Crunch simulations. Higher values of reaction rates caused an irreversible collapse of the time step in the version of Crunch used in this study. This difficulty is now overcome in the subsequent versions of Crunch. In kinetic simulations run with Hytec, kinetic rates were set to 4 10^{-8} mol.m^{-2}.s^{-1} (resp. 3 10^{-8} mol.m^{-2}.s^{-1}) for portlandite (resp. Ca-oxalate) and the specific surface area A_s to 1 m^2.g$^{-1}_{mineral}$ for both minerals. The solubility of portlandite is 2 10^{-2} mol.L^{-1} of solution at pH~12.5. As the porosity is ω~0.2, the solubility of portlandite is thus C~4 mol.m^{-3} of porous medium at pH~12.5. The timescale of chemical transfer is thus given by the expression:

$$\Delta t_3 = \frac{C}{k_{rate} S} \sim 400\ s\text{, for Crunch and } \Delta t_3 \sim 45\ s\text{, for Hytec} \qquad (15)$$

Note however that the solubility of portlandite may be significantly increased in case of pH perturbation and thus could potentially lead to much higher chemical transfer characteristic times. Also, clogging may induce local concentration of flow lines with higher Darcy velocities and thus shorten characteristic transport times. This shows that, for simulations run in kinetic mode, although the characteristic time for portlandite dissolution is rather small, an overlap between characteristic times for transport and chemistry is possible during the course of the simulated experiment.

Calculations were conducted on a UNIX work-station for Hytec v.3.5.6 and in DOS environment for Crunch v.2006 (in both cases Pentium IV 3.2 GHz). Duration of calculation ranged from 1 to 6 hours. Post processing was performed using Tecplot®, MSExcel® and Hype®, a tool dedicated to Hytec.

4. Results of simulations

In a first stage (§4.1), the initial fluid velocity fields computed by Hytec and Crunch are compared; spatial profiles of non reactive tracers transported under stationary flow conditions

are also compared. The evolution of the reactive system without porosity update is then simulated (§4.2). Finally (§4.3), results of Crunch and Hytec simulations taking into account processes coupled with porosity variations are compared. Focus is placed in this presentation on the evolution during the simulated experiment of precipitate, permeability, porosity and velocity fields.

4.1. Stationary hydraulic and non-reactive transport of species

411. Steady state hydraulics

Profiles of the x- and y-components of the initial Darcy velocities are recorded on a line located in the middle of the box (Line 1 in Figure 1) and presented in Figure 2 for Crunch and Hytec simulations.

The x-component value of the Darcy velocity (U_x) progressively increases from the left to the right side of the cell, from 0 to 10^{-7} m.s^{-1}, except in the region of the portlandite wall where the velocity remains constant. Finally, U_x decreases, as expected, and it reaches zero on the chamber boundaries. U_y presents negative values in front of the portlandite wall and positive values behind this wall. Steep transitions are observed between the portlandite wall and the rest of the chamber as a result of the difference in permeability values between these regions (one order of magnitude initially). Crunch and Hytec velocity fields can be considered identical except for few points located behind the portlandite wall for which the differences remain low (<10%). Analogous profiles, not shown here, indicate that Hytec and Crunch flow fields are very similar whatever the line considered.

412. Dispersion and diffusion of non reactive tracers

The transport of a tracer in the initial steady state flow velocity field presented in §4.1.1 was computed with Crunch and Hytec as a further elementary test. A solution containing an inert species is continuously injected in the box by Inlet 2 (Figure 1) with a total concentration of 1 µmolal. Spatial profile of the tracer concentration is recorded on Line 1 (Figure 1) during 3 days. The concentration profiles (Figure 3) obtained with Hytec and Crunch are almost superposed for each time considered. The most significant difference between the two codes is observed for points located at the extreme left of the box (low X-coordinates), but remains less than 10%. Analogous profiles, not shown here, indicate that the dispersion recorded with Hytec and Crunch is very similar whatever the line considered.

These preliminary studies (§4.1.1 and §4.1.2) show that initial flow fields computed by Crunch and Hytec are very similar and that concentration profiles of a tracer transported and dispersed in this flow field are also very close. In the following sections, the complete experiment involving dissolution and precipitation, first with a constant porosity and then with porosity update is set up and simulated with both codes.

4.2. Simulation of the complete experiment with fixed porosity

In this set of simulations, the 2D experiment described in §2 is simulated without an update of the porosity and permeability fields, which therefore retain their initial values. Injection of oxalate ions by Inlet 2 (Figure 1) leads to massive precipitation of calcium oxalate in the region where a high calcium source term is located, i.e. at the location where portlandite is initially present (Q2 region). When this local solid state calcium source is consumed, the newly formed calcium oxalate begins to dissolve because the injected fluid contains no

dissolved calcium (Table 2) and is therefore undersaturated with respect to calcium oxalate. Under these conditions, the obstacle created by the precipitation of calcium oxalate is expected to perforate. Figure 4 and Figure 5 present the variation with time of the portlandite and Ca-oxalate volume fraction simulated with Crunch (upper row) and Hytec (local equilibrium hypothesis, lower row). The portlandite begins to dissolve at the upper part of the wall and is replaced by the Ca-oxalate as shown in Figure 5. Figure 4 and Figure 5 show relatively good agreement between Crunch and Hytec for the portlandite dissolution process. Slight differences are however visible with respect to the Ca-oxalate precipitation: i) the maximum Ca-oxalate volume fraction precipitated is higher (~29 %) for Crunch than for Hytec (~26 %), ii) the spatial distribution of the Ca-oxalate precipitate is more spread out in the Hytec results than in Crunch. The perforation of the calcium oxalate wall is also predicted to occur sooner with Crunch (55 days) than with Hytec (90 days).

Figure 6.a shows the variation with time of mineral concentrations cumulated over the entire chamber during the experiment described above. As previously noticed in Figure 4, portlandite dissolution is similar for Crunch (dotted line) and Hytec (continuous line) with an exponential-like decrease. During the first 20 days, the integral precipitation of calcium oxalate over the chamber is equivalent for both simulations. After this time, the total Ca-oxalate concentration becomes lower with Crunch, with a maximum concentration reached earlier.

Note that the maximum time step was constrained for both codes to the same value (40 seconds) and that both codes reached this time step value. Effects of maximum time step values will be briefly presented in the discussion section.

4.3. Simulation of the complete experiment with porosity and permeability update

As in the case with the simulations presented earlier, injection of the oxalate rich fluid leads to the transformation of the portlandite rich zone into a calcium oxalate wall in simulations in which porosity and permeability are updated. Because of the large increase in mineral volumes in reaction (1) and following porosity update, this wall will now divert significantly the flow lines. Major results obtained with Hytec (equilibrium hypothesis) and Crunch are displayed on Figure 6 to Figure 11. As previously, the maximum time step was constrained to the same value (40 seconds), which was reached by both codes. In both cases, portlandite dissolution (Figure 6.b and Figure 7) proceeds quite regularly from the top left in about the same time. Note however that the last remainder of portlandite is not located at the same part of the wall (in the middle for Crunch and at the bottom for Hytec, see Figure 7). Hytec and Crunch results display significant differences in the way the oxalate wall (Figure 8 and Figure 9) and the associated flow-fields evolve. First, the wall perforation occurs after ~50 days for Crunch, whereas this event happens after only ~80 days for Hytec. Both codes predict a perforation localized at the top of the box. It is also clear that in the Crunch simulations, the conversion of portlandite to Ca-oxalate builds a much more impermeable obstacle than in Hytec simulations (Figure 10 and Figure 11), leading to a much stronger diversion of flow lines (Figure 8 and Figure 9). This is consistent with the higher concentration level reached by Ca-oxalate in Crunch results (> 28.1 vol. %) by comparison to Hytec (~25.5 vol. %). The integrated volume fraction of portlandite dissolved during this experiment (Figure 6.b) is very similar for both predictions, displaying an almost linear variation. For Ca-oxalate, the maximum reached is lower with Crunch, but happens for both codes after 40 days.

The permeability profile along a vertical line (Line 2) situated in the oxalate wall (Figure 10) tends towards a nearly constant value before perforation in Hytec simulations, whereas a

significant difference in permeability always exists between the bottom and the upper part of this line in Crunch runs. The curve rebound observed in Crunch permeability profiles is due to the existence of a preserved island of portlandite. Very low permeabilities (~10^{-18} m^2, locally) are obtained with Crunch after 70 days. A comparison of the temporal evolution of the porosity near the upper part of the Ca-oxalate wall (Figure 11) shows indeed that minimum porosities obtained with Crunch (~ 1 %) are much lower than for Hytec (~5 %).

Finally, it should be noted, that very low concentrations of Ca-oxalate and portlandite are predicted in both Crunch and Hytec simulations to form as a result of precipitation after about 1 month in the region between the portlandite obstacle and the outlet.

5. Discussion

Preliminary tests dealing with pure transport show that predictions by Hytec and Crunch of the advection, diffusion and dispersion of an inert species in the initial velocity field are in very good agreement. Some minor local differences (never above 10%) were found and could be attributed to a difference in the numerical dispersion in both codes. Although these discrepancies are small, they have to be kept in mind as possible sources of divergence in the global results.

The test in which the experiment was simulated without porosity update (§4.2, Figure 4, Figure 5 and Figure 6.a) provides other clues to explain the differences in the predictions of the complete (fully coupled) experiment. The portlandite spatial distribution (Figure 4) is very similar for the two codes. The exponential decrease in the global portlandite quantity in the chamber with time (Figure 6.a), in a fashion similar to what occurs in a stirred tank reactor, is also very similar for Crunch and Hytec (total dissolution in ~75 days). In contrast, the spatial distribution of oxalate (Figure 5) displays significant differences after 20 days, even if at this

time the integrated quantity of precipitated oxalate is the same for Crunch and Hytec (Figure 6.a). Although the scenario is qualitatively similar for both tools, the wall perforation happens much sooner in Crunch predictions. The local maximum concentration of oxalate is much higher in Crunch simulations (~ 28%) than for Hytec (~25%). Porosity and permeability being constant in this computation, the disparities observed here are thus related to the kinetic description of mineral dissolution/precipitation processes in Crunch. Careful examination of the integral curves (Figure 6.a), shows that a part of the calcium initially contained in portlandite never precipitates and escapes at the outlet. In the case of Crunch, this fraction of non precipitated calcium, escaping as dissolved species in solution, is one and a half larger than in Hytec. This is consistent with a limitation of precipitation in Crunch due to kinetics. Attempts were made to simulate this configuration, i.e. with no porosity update, using the kinetic mode of Hytec. The rate constant was given for portlandite and Ca-oxalate the value $\pm 10^{-5}$ $mol.m^{-2}.s^{-1}$ with 1 $m^2.g^{-1}$ of specific area. Kinetic runs performed with Hytec in these conditions gave results very close from the local equilibrium case, as well for portlandite and oxalate distributions. Other tests were made with Hytec in kinetic mode with a range of rate constants; however because of the fundamentally differing surface area norms of Hytec and Crunch (Table 5), it was never possible to simulate completely equivalent systems.

It can be concluded from computations performed with this configuration that assumptions on variations of mineral surface area during the course of dissolution and precipitation has a major impact on flow pattern predictions. This seems to be specifically important for secondary mineral species for which the initial surface area is ill-defined, as well as the transition from precipitation to redissolution which is treated in different ways by the simulation tools. The local differences in spatial distribution of the oxalate (e.g. very high local concentrations with Crunch) are a specific feature that seems to be linked to the surface area models.

The simulations, in which porosity is updated (from Figure 6.b to Figure 11), show for both Crunch and Hytec that the overall portlandite dissolution is faster (total dissolution after 40 days) than in the case with fixed porosity (Figure 6). The main difference in results remains that, in the case of Crunch simulations, an island of portlandite is temporarily protected from the aggressive solution as a result of the formation of a hermetic layer of Ca-oxalate. The faster dissolution is explained by the fact that the injected flow of dissolved oxalate is diverted by porosity evolution towards zones where portlandite dissolution is less advanced. So, local porosity reduction leads to a faster flushing of the experimental chamber with the oxalate containing solution and consequently to a faster and linear consumption of the portlandite mineral (Figure 6.b) instead of an exponential decrease. The integral curves (Figure 6.b) show in addition that the available calcium is more efficiently precipitated than in the fixed porosity case (Figure 6.a). Nevertheless, calcium escapes in greater quantity from the reaction chamber for the Crunch simulation in kinetic mode, which is physically correct.

The Ca-oxalate mineral distribution differs considerably between both predictions (Figure 8 and Figure 9). Whereas the integrated volume fraction of Ca-oxalate over the chamber is lower in Crunch than in Hytec predictions, the minimum porosity with Crunch reaches 0.3%, compared to the ~5% obtained with Hytec. As previously discussed, such differences in the Ca-oxalate distribution most probably originate from the surface area model used. Therefore, the permeability decreases strongly (Figure 10), leading to a considerably higher coupling effect with flow in the case of Crunch. Another difference between codes concerns the permeability laws (see section 3.1). However, the differences in permeability models cannot explain these discrepancies, which have already been noted for simulations without porosity update.

In order to reproduce Crunch results with Hytec in kinetic mode, a qualitative analysis of the different rate limiting processes was conducted. If initial conditions of the porous medium are considered (i.e. 11 vol. % of portlandite in the obstacle, 19 vol.% porosity), complete conversion of the portlandite into Ca-oxalate should lead to a residual porosity of 8 vol.%. Both codes predict minimal porosities that are significantly lower than this value, which is based on a scenario in which calcium would locally precipitate (Figure 11). In addition, the Ca-oxalate precipitation at node N (Figure 1 and Figure 11), a point located far at the back of the obstacle, starts earlier in Crunch kinetic simulations than with Hytec at equilibrium. Among processes that potentially regulate the localization and concentration of the oxalate precipitate, the following were identified as the most relevant ones:

- The influx of the fresh oxalate solution and its diversion by porosity reduction.
- The precipitation rate of Ca-oxalate. If this rate is too large, calcium dissolved from portlandite will not be able to be transported before precipitation and oxalate ions will also be immobilized locally.
- The dissolution rate of portlandite. If this rate is too small, too much dissolved oxalate will escape from the portlandite zone.
- The magnitude of the diffusion-dispersion coefficients.

Because of the large number of parameters and of the duration of computation, it was not possible to perform an exhaustive sensitivity analysis. A specific focus was given to the values of dissolution/precipitation rate constants and particularly to the observation that, as noted above, transport of calcium before immobilization requires a relatively slower precipitation rate for Ca-oxalate than the corresponding dissolution rate of portlandite. It was indeed found that some of the features observed in Crunch results could be reproduced with Hytec in kinetic mode when the dissolution rates of portlandite was set to $-4\ 10^{-8}$ $mol.m^{-2}.s^{-1}$ (1 $m^2.g^{-1}$) and the dissolution/precipitation rate of Ca-oxalate to $\pm 3\ 10^{-8}$ $mol.m^{-2}.s^{-1}$ (1 $m^2.g^{-1}$).

For instance, minimum local porosities were lower (~3 % instead of ~5 %) and the perforation of the Ca-oxalate wall occurred after ~60 days, instead of ~80 days with Hytec at equilibrium (see §4.2). The evolutions at node N were also more consistent (Figure 12). Nevertheless, very low porosities as obtained in Crunch results could not be reached. These trials with Hytec in kinetic mode show that some important rate limiting factors controlling the spatial distribution of Ca-oxalate have been identified, but that a precise match of simulation results is presently not achievable because of the different models taken for surface area evaluation in the codes.

Reaching very low porosities also results in a stronger coupling between chemistry and flow in Crunch simulations because of the cubic expression taken by the permeability (equations (3) and (9)). It was found that, due to this stronger coupling, Crunch results were more sensitive than Hytec to the maximum time step allowed during the run, especially because the code is non-iterative. Simulations performed only with the smallest time step tested in Crunch are presented here, but a sensitivity study was actually made on this parameter. For higher maximum time step, the wall perforation occurs later in time but equivalent quantitative differences still exist in the localization of the precipitates. The sensitivity of the results to the time step used in Crunch reflects the way in which the code handles the updating of mineral volume fractions (and thus, porosity and permeability). Because the mineral concentrations are only updated at the end of the time step, rather than computed implicitly within a time step; the time step should be calculated such as it does not overshoot the available mineral volume fractions.

Future development of this project will follow two major lines:

i) The present study has stressed the influence of the evolution of parameters such as the surface area as a function of the reaction progress. It led to the development in Hytec

(v.3.7) and Crunch (v2007) of a much larger set of reactive surface area models. Their implementation will make it possible to describe reactive porous media with a sounder scientific basis and will also allow for analytically equivalent comparison between codes. The sensitivity of predictions to spatial discretization will also be assessed by increasing the resolution of the discretization of the chamber.

ii) The design of the future laboratory experiment can now be considered as sufficiently mature. Although providing different results, predictions show that the time scale of cementation/perforation processes is comparable for both codes. The simulations also show that an acute description of the kinetics of precipitation and redissolution of the secondary mineral Ca-oxalate (in particular the surface area dependence of these successive processes) is crucial to explain and discriminate the predicted flow patterns. The acquisition of this rate law can be seen as a preliminary stage on the roadmap leading to the coupled 2D experiment. Several technical challenges have also to be overcome in order to construct the experimental design. A first difficulty will be met when dealing with solution density, because the oxalate rich fluid injected in the box is higher in density than pure water in equilibrium with portlandite. Such a difficulty can be overcome by initially filling the box with an appropriate electrolyte to minimize the density contrast. Also the initial filling of the reaction chamber will be a technically difficult operation: spatial heterogeneities (particularly in the portlandite wall) can be the cause of unexpected instabilities in the permeability evolution. The mechanical behavior of the variably consolidated quartz sand mixed with secondary precipitate could in addition restrict the range of initial portlandite enrichment in the central part of the reactor. Monitoring and time analysis of pressure drop signals are thus important tools that need to be included in the complete experimental design. Among other achievements necessary to succeed in such an experiment, innovative

tracer techniques will be essential. In particular, a real-time tracking of mineral dissolution and precipitation processes inside the reaction chamber is desirable. The present idea for recording the mineral evolution within the chamber is to co-precipitate trace elements (Ba, Sr …), possibly as radioactive tracers, in the newly formed Ca-oxalate phase. The feasibility of forming such solid solutions, however, requires additional research.

Models that link texture and porosity are not well developed in the present state of the art in reactive transport codes. Approaches aiming at describing in a mechanistic way fluid flow and reactions in an individual pore have been explored by several teams (Adler et al. [31-34]; Scholes et al. [35]). The Comedie2D experiment will hopefully help to fill some of the gap between these microscopic approaches and larger scale reactive transport models.

6. Conclusions

Simulations of physical transformations occurring in porous media involving significant variations of porosity coupled to chemical transformations and flow were explored in a two-dimensional reactor by using two different reactive transport modelling tools, Hytec and Crunch.

Predictions by these two codes of the evolution in time of the spatial precipitate distributions are in qualitative agreement, although the internal models and algorithms used by the two codes are different.

The most important discrepancies between Crunch and Hytec results are found to be related to the surface area models used to describe the dissolution/precipitation of secondary minerals (Ca-oxalate in the present study) and more generally to the kinetic description of such secondary precipitation processes. This observation pinpoints the importance of properly

describing and simulating the way the texture evolves in porous medium when porosity undergoes significant variations. In particular, the use of a chemical equilibrium assumption in modeling systems with strong cementation is questionable, since reactive surface areas markedly decrease and should thus limit reaction rates.

In order to progress further into the preparation of this experiment and associated numerical benchmarking, Hytec and Crunch are presently modified in order to include an extended set of surface area models. The numerical benchmarking will also be extended to a third numerical tool, the ALLIANCES platform [36, 37].

Acknowledgements

This work was supported by the CEA Nuclear Energy Direction. We also acknowledge members of the PGT (Pôle Géochimie Transport, Armines-CEA-EDF-IRSN-Lafarge-Total) for fruitful discussions. Crunch development was supported by the Director, Office of Science, Office of Basic Energy Sciences, Division of Chemical Sciences, Geosciences, and Biosciences of the U.S. Department of Energy under Contract No. DE-AC02-05CH11231 to Lawrence Berkeley National Laboratory. The authors also acknowledge three anonymous reviewers for their very constructive comments.

References

1. Bildstein, O., et al., *Modelling iron-clay interactions in deep geological disposal conditions.* Physics and Chemistry of the Earth, 2006. **31**(10-14): p. 618-625.
2. Trotignon, L., et al., *Predicting the long term durability of concrete engineered barriers in a geological repository for radioactive waste.* Physics and Chemistry of the Earth, 2007. **32**(1-7): p. 259-274.
3. Li, L., C.H. Benson, and E.M. Lawson, *Modeling porosity reductions caused by mineral fouling in continuous-wall permeable reactive barriers.* Journal of Contaminant Hydrology, 2006. **83**(1-2): p. 89-121.
4. Wagner, R., et al., *Numerical simulation of pore space clogging in geothermal reservoirs by precipitation of anhydrite.* International Journal of Rock Mechanics and Mining Sciences, 2005. **42**(7-8): p. 1070-1081.
5. Le Gallo, Y., O. Bildstein, and E. Brosse, *Coupled reaction-flow modeling of diagenetic changes in reservoir permeability, porosity and mineral compositions.* Journal of Hydrology, 1998. **209**(1-4): p. 366-388.
6. Pape, H., et al., *Anhydrite cementation and compaction in geothermal reservoirs: Interaction of pore-space structure with flow, transport, P-T conditions, and chemical reactions.* International Journal of Rock Mechanics and Mining Sciences, 2005. **42**(7-8): p. 1056-1069.
7. Mikutta, C., F. Lang, and M. Kaupenjohann, *Soil organic matter clogs mineral pores: Evidence from H-1-NMR and N-2 adsorption.* Soil Science Society of America Journal, 2004. **68**(6): p. 1853-1862.
8. VanGulck, J.F. and R.K. Rowe, *Influence of landfill leachate suspended solids on clog (biorock) formation.* Waste Management, 2004. **24**(7): p. 723-738.
9. Suliman, F., et al., *Change in flow and transport patterns in horizontal subsurface flow constructed wetlands as a result of biological growth.* Ecological Engineering, 2006. **27**(2): p. 124-133.
10. van der Lee, J., et al., *Module-oriented modeling of reactive transport with HYTEC.* Computers & Geosciences, 2003. **29**(3): p. 265-275.
11. Yeh, G.T., M.D. Siegel, and M.H. Li, *Numerical modeling of coupled variably saturated fluid flow and reactive transport with fast and slow chemical reactions.* Journal of Contaminant Hydrology, 2001. **47**(2-4): p. 379-390.
12. Steefel, C.I., D.J. DePaolo, and P.C. Lichtner, *Reactive transport modeling: An essential tool and a new research approach for the Earth sciences.* Earth and Planetary Science Letters, 2005. **240**(3-4): p. 539-558.
13. Lagneau, V., *Influence des processus géochimiques sur le transport en milieu poreux ; application au colmatage de barrières de confinement potentielles dans un stockage en formation géologique.* 2000, Ph. D. from Ecole des Mines de Paris: Fontainebleau, France.
14. Trotignon, L., et al., *Design of a 2-D cementation experiment in porous medium using numerical simulation.* Oil & Gas Science and Technology-Revue De L Institut Francais Du Petrole, 2005. **60**(2): p. 307-318.
15. Steefel, C.I., *Crunch - Users Guide*. 2006, Lawrence Berkeley Laboratory, USA.
16. Cross, J.E. and F.T. Ewart, *Hatches - a Thermodynamic Database and Management-System.* Radiochimica Acta, 1991. **52-3**: p. 421-422.
17. Lide, D.R., *Vapor-Liquid-Equilibrium Database.* Journal of Chemical Information and Computer Sciences, 1994. **34**(3): p. 690-690.

18. Morel, E.H. and A.B. Birtles, *Optimization of Groundwater Abstraction from a Coastal Aquifer*. Hydrological Sciences Journal-Journal Des Sciences Hydrologiques, 1983. **28**(1): p. 169-182.
19. Yeh, G.T. and V.S. Tripathi, *A Model for Simulating Transport of Reactive Multispecies Components - Model Development and Demonstration.* Water Resources Research, 1991. **27**(12): p. 3075-3094.
20. Steefel, C.I. and K.T.B. MacQuarrie, *Approaches to modeling of reactive transport in porous media.* Reactive Transport in Porous Media, 1996. **34**: p. 83-129.
21. Van der Lee, J., *Modelling of transport and geochemical behaviour of radionuclides in presence of colloides, Ph. D.* 1997, Ph. D. from Ecole des Mines de Paris: Fontainebleau, France.
22. Van der Lee, J., *Reactive transport modelling with HYTEC Users guide and tutorial*. 2005, Technical report LHM/RD/05/30: Ecole des Mines de Paris.
23. Salles, J., J.F. Thovert, and P.M. Adler, *Reconstructed Porous-Media and Their Application to Fluid-Flow and Solute Transport.* Journal of Contaminant Hydrology, 1993. **13**(1-4): p. 3-22.
24. Colston, B.J. and V.J. Robinson, *Ionic-Strength Effects in Modeling Radionuclide Migration in Environmental Systems - Estimating the Errors and Uncertainties.* Journal of Environmental Radioactivity, 1995. **29**(2): p. 121-136.
25. De Windt, L., et al., *Intercomparison of reactive transport models applied to UO2 oxidative dissolution and uranium migration.* Journal of Contaminant Hydrology, 2003. **61**(1-4): p. 303-12.
26. Lagneau, V., *R2D2 - Reactive transport and waterflow on an odd dimension 2 grid*. 2003, Rapport technique LHM/RD/03/05: Ecole des Mines de Paris.
27. Yabusaki, S., et al., *Multicomponent reactive transport in an in situ zero-valent iron cell.* Environmental Science & Technology, 2001. **35**(7): p. 1493-1503.
28. Gupta, A.D., et al., *High-Resolution Monotonic Schemes for Reservoir Fluid-Flow Simulation.* In Situ, 1991. **15**(3): p. 289-317.
29. Steefel, C.I. and A.C. Lasaga, *A Coupled Model for Transport of Multiple Chemical-Species and Kinetic Precipitation Dissolution Reactions with Application to Reactive Flow in Single-Phase Hydrothermal Systems.* American Journal of Science, 1994. **294**(5): p. 529-592.
30. Wang, Y. and P. Van Cappellen, *A multicomponent reactive transport model of early diagenesis: Application to redox cycling in coastal marine sediments* Geochimica et Cosmochimica Acta, 1996. **60**(16): p. 2993-3014.
31. Adler, P.M. and B. Berkowitz, *Effective medium analysis of random lattices.* Transport in Porous Media, 2000. **40**(2): p. 145-151.
32. Borisova, E.A. and P.M. Adler, *Deposition in porous media and clogging on the field scale.* Physical Review E, 2005. **71**(1): p. 1-19.
33. Valfouskaya, A. and P.M. Adler, *Nuclear-magnetic-resonance diffusion simulations in two phases in porous media.* Physical Review E, 2005. **72**(5): p. 1-11.
34. Valfouskaya, A., et al., *Nuclear magnetic resonance diffusion with surface relaxation in porous media.* Journal of Colloid and Interface Science, 2006. **295**(1): p. 188-201.
35. Scholes, O.N., et al., *Permeability anisotropy due to consolidation of compressible porous media.* Transport in Porous Media, 2007. **68**(3): p. 365-387.
36. Bengaouer, A., et al., *ALLIANCES: Simulation platform for radioactive waste disposal.* Atw-International Journal for Nuclear Power, 2005. **50**(8-9): p. Xiii-Xiv.
37. Montarnal, P., et al., *Presentation and use of a reactive transport code in porous media.* Physics and Chemistry of the Earth, 2007. **32**(1-7): p. 507-517.

Table captions

Table 1: Properties of the different regions (Q1, Q2 and Q3, see Figure 1) of porous medium after the first steps of dimensioning.

Table 2: Definition of solution chemistry and boundary Darcy velocity for inlet 1 and 2.

Table 3: Equilibrium constants for all the considered reactions. The experiment is simulated at a constant temperature (25°C).

Table 4: Main differences between Hytec and Crunch concerning models for diffusion and intrinsic permeability variations with porosity.

Table 5: Main differences between Hytec and Crunch concerning models for kinetics and reactive surface area. Parameter values for Crunch were A_{bulk} = 1000 m^2/m^3 and k_{rate} = $\pm 10^{-5}$ $mol.m^{-2}.s^{-1}$. For Hytec, k_{rate} ranging from $\pm 10^{-5}$ $mol.m^{-2}.s^{-1}$ to $\pm 10^{-9}$ $mol.m^{-2}.s^{-1}$ were tested, A_s = 1 $m^2.g^{-1}$, nucleus = 1 $m^2.m^{-3}_{solution}$.

Figure captions

Figure 1: Schematic view of the experimental set-up from *Trotignon et al.* study [14]. The set-up is a square (14 cm of edge size) composed of quartz grains except for a zone (Q2) composed of quartz and portlandite grains (2 cm of width). Lines labeled 'Line 1' (y=7.0 cm) and 'Line 2' (x=9.5 cm) (resp. node 'N' (x=9.5 cm; y=10.8 cm)) are test lines (resp. test node) on which specific profiles will be compared.

Figure 2: Linear profiles of x-component (a) and y-component (b) of Darcy velocity with Crunch (bold line) and Hytec (symbols) recorded on Line 1.

Figure 3: Concentration profiles of 'Tracer' injected by inlet 2 recorded on Line 1 with Hytec (symbols) and Crunch (lines) during the first 3 days.

Figure 4: Evolution of portlandite volume fraction simulated with Crunch (upper row) and Hytec (lower row) after 5 days (a), 20 days (b) and 50 days (c) without porosity update.

Figure 5: Evolution of calcium oxalate volume fraction simulated with Crunch (upper row) and Hytec (lower row) after 5 days (a), 20 days (b) and 50 days (c) without porosity update.

Figure 6: Variation with time of the summed concentration of portlandite and Ca-oxalate over the entire reaction chamber simulated with Crunch (continuous lines) and Hytec (dotted lines) without porosity update (a) and with porosity update (b).

Figure 7: Evolution of portlandite volume fraction with time (5, 10, 30 and 40 days from the left to the right) with porosity update. The upper row presents Crunch results and the lower one is Hytec's results.

Figure 8: Evolution of Ca-oxalate volume fraction and flow rate fields with time (10, 20, 40and 70 days) predicted with Crunch with porosity update.

Figure 9: Evolution of Ca-oxalate volume fraction and flow rate fields with time (10, 40, 70 and 90 days) predicted with Hytec with porosity update.

Figure 10: Permeability variation during the experiment simulated with Crunch (a) and Hytec (b) on a vertical line located in the clogging obstacle (see Line 2 in Figure 1).

Figure 11: Temporal profiles of porosity (a) and mineral volume fraction (b) recorded on node N (see Figure 1) predicted with Hytec (equilibrium hypothesis, white symbols) and Crunch (dark symbols).

Figure 12: Temporal profiles of porosity (a) and mineral volume fraction (b) recorded on node N (see Figure 1) predicted with Hytec (kinetic hypothesis, white symbols) and Crunch (dark symbols).

Table 1

	Q1	Q2	Q3
Width (X-axis) (mm)	80	20	40
Initial porosity ω_0	0.3	0.19	0.3
Initial permeability ($m.s^{-1}$)	$1.0\ 10^{-5}$	$1.64\ 10^{-6}$	$1.0\ 10^{-5}$
Dispersivity α (mm)	20	20	20
Initial effective diffusion coefficient D_0 ($m^2.s^{-1}$)	$1.0\ 10^{-9}$	$1.0\ 10^{-9}$	$1.0\ 10^{-9}$
Storage coefficient (m^{-1}) *(not specified with Crunch)*	$1.0\ 10^{-2}$	$1.0\ 10^{-2}$	$1.0\ 10^{-2}$
Quartz concentration ($molal_{solution}$)	102.8	196	102.8
Portlandite concentration ($molal_{solution}$)	0	17.51	0
Initial pH	6.8	12.5	6.8

Table 2

	Inlet 1	Inlet 2
pH	6.8	6.8
Na^+ (total) molal	0.02	0.8
Ca^{2+} (total) molal	0	0
Cl^- (total) molal	0.02	0
$C_2O_4^{2-}$ (total) molal	0	0.4
Darcy velocity vector (U_x, U_y) $m.s^{-1}$	($2\ 10^{-7}$, 0)	(0, $4\ 10^{-7}$)

Table 3

Reaction	$Log_{10}K$ (25°C)
$CaC_2O_4.H_2O \leftrightarrow Ca^{2+} + C_2O_4^{2-} + H_2O$	-8.63
$Ca(OH)_{2\,(aq)} + 2H^+ \leftrightarrow Ca^{2+} + 2\,H_2O$	22.55
$H_2C_2O_{4\,(aq)} \leftrightarrow 2\,H^+ + C_2O_4^{2-}$	-5.42
$HC_2O_4^- \leftrightarrow H^+ + C_2O_4^{2-}$	-4.19
$CaC_2O_{4\,(aq)} \leftrightarrow Ca^{2+} + C_2O_4^{2-}$	-3.00
$Ca(C_2O_4)_2^{2-} \leftrightarrow Ca^{2+} + 2\,C_2O_4^{2-}$	-8.1
$Ca(C_2O_4)_3^{4-} \leftrightarrow Ca^{2+} + 3\,C_2O_4^{2-}$	-8.2
$NaC_2O_4^- \leftrightarrow Na^+ + C_2O_4^{2-}$	-1
$CaCl^+ \leftrightarrow Ca^{2+} + Cl^-$	0.29
$CaCl_{2\,(aq)} \leftrightarrow Ca^{2+} + 2\,Cl^-$	0.64
$CaOH^+ + H^+ \leftrightarrow Ca^{2+} + H_2O$	12.83
$NaCl_{\,(aq)} \leftrightarrow Na^+ + Cl^-$	0.78
$NaOH_{\,(aq)} + H^+ \leftrightarrow Na^+ + H_2O$	14.2
$HCl_{\,(aq)} \leftrightarrow H^+ + Cl^-$	0.71

Table 4

	HYTEC	CRUNCH
Diffusion laws *(m^2/s)*	Archie's modified law: $D = D_e(\omega_0)\left(\frac{\omega - \omega_c}{\omega_0 - \omega_c}\right)^a$ *$D_e(\omega_0)$: effective diffusion coefficient* *See text for parameters*	$D = \frac{D_0}{F}$, *D : effective diffusion coefficient* *D_0 : molecular diffusion coefficient* *F: Formation factor* $F = \omega^{-m}$ *m: cementation coefficient*
Permeability laws *(m^2)*	Kozeny-Carman modified equation: $k_s = k_0\left(\omega/\omega_0\right)^3\left[\frac{1-\omega_0}{1-\omega}\right]^2$	$k_s = k_0\left(\omega/\omega_0\right)^3$

Table 5

HYTEC	CRUNCH
Local Equilibrium	
Infinite surface area whatever the porosity	Not available in the current version
Kinetics	
$r_s = -A_s k_{rate}\left[1-\left(\frac{Q_s}{K}\right)\right]$ *r_s:dissolution/precipitation reaction rate* *k_{rate}: dissolution/precipitation rate constant* *(in Hytec, k_{dissol} and k_{precip} may take different values)* *Q_s: ion activity product* *K: equilibrium constant* *A_s: specific surface area*	
- A_{bulk} ($m^2.m^{-3}_{solution}$) Hypothesis of homogeneous, mono-disperse suspension of spherical particles: $A_s = 3/\rho r$ *and* $A_{bulk} = A_s C$ *C: particle concentration* *ρ: particle density* *r: radius of spherical particle (supposed constant)*	**- A_{bulk} ($m^2.m^{-3}_{porous\ medium}$)** $A_s = A_{bulk} V_m / \omega_m MW_m$, *V_m: molar volume of the solid phase* *ω_m: porosity* *MW_m: molar weight of the phase* $A_{bulk} = A_{bulk,0}\begin{cases}\left[\left(\frac{\omega}{\omega_0}\right)\left(\frac{\phi_m}{\phi_{m,0}}\right)\right]^{2/3} & dissolution\\ \left[\frac{\omega}{\omega_0}\right]^{2/3} & precipitation\end{cases}$ *ϕ_m: mineral volume fraction* *$\phi_{m,0}$: initial mineral volume fraction* For secondary minerals: $\phi_{m,0} = 0.01$
- A_s ($m^2.g^{-1}_{mineral\ phase}$ or $m^2.mol^{-1}_{mineral\ phase}$) A nucleus is defined in $m^2.m^{-3}_{solution}$ to make possible secondary mineral precipitation	**- A_s ($m^2.g^{-1}_{porous\ medium}$)** $A_{bulk} = \begin{cases}\phi_m A_s MW_m / V_m & dissolution\\ A_{bulk,0}\left[\frac{\omega}{\omega_0}\right]^{2/3} & precipitation\end{cases}$ For secondary minerals: $A_{bulk,0} = 100\ m^2.m^{-3}$

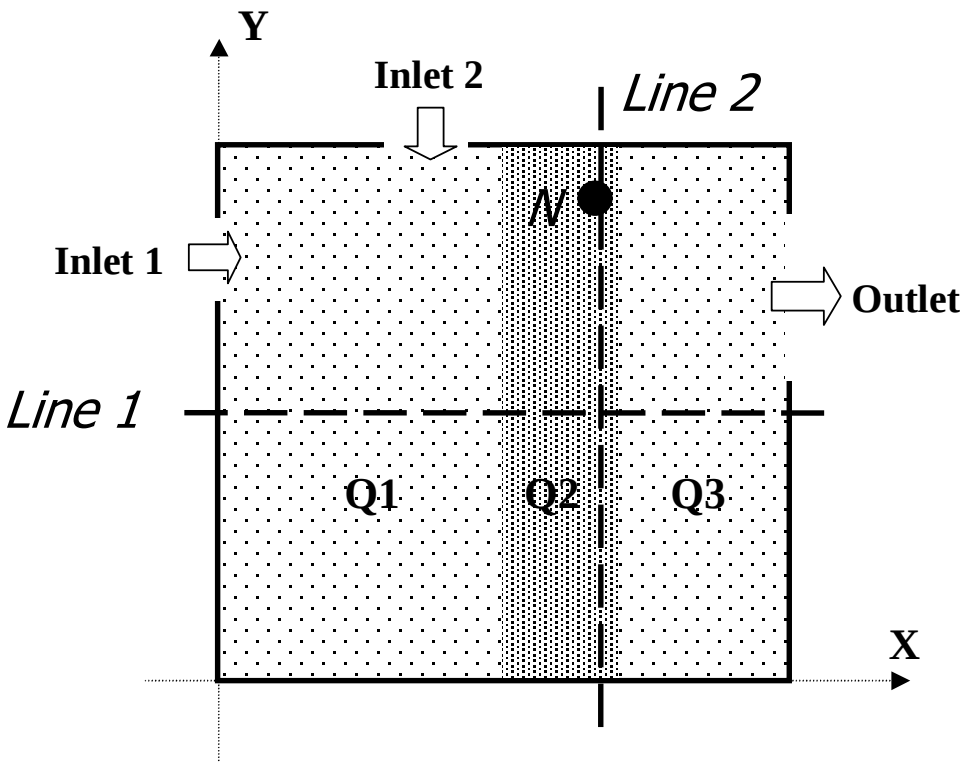

Figure 1

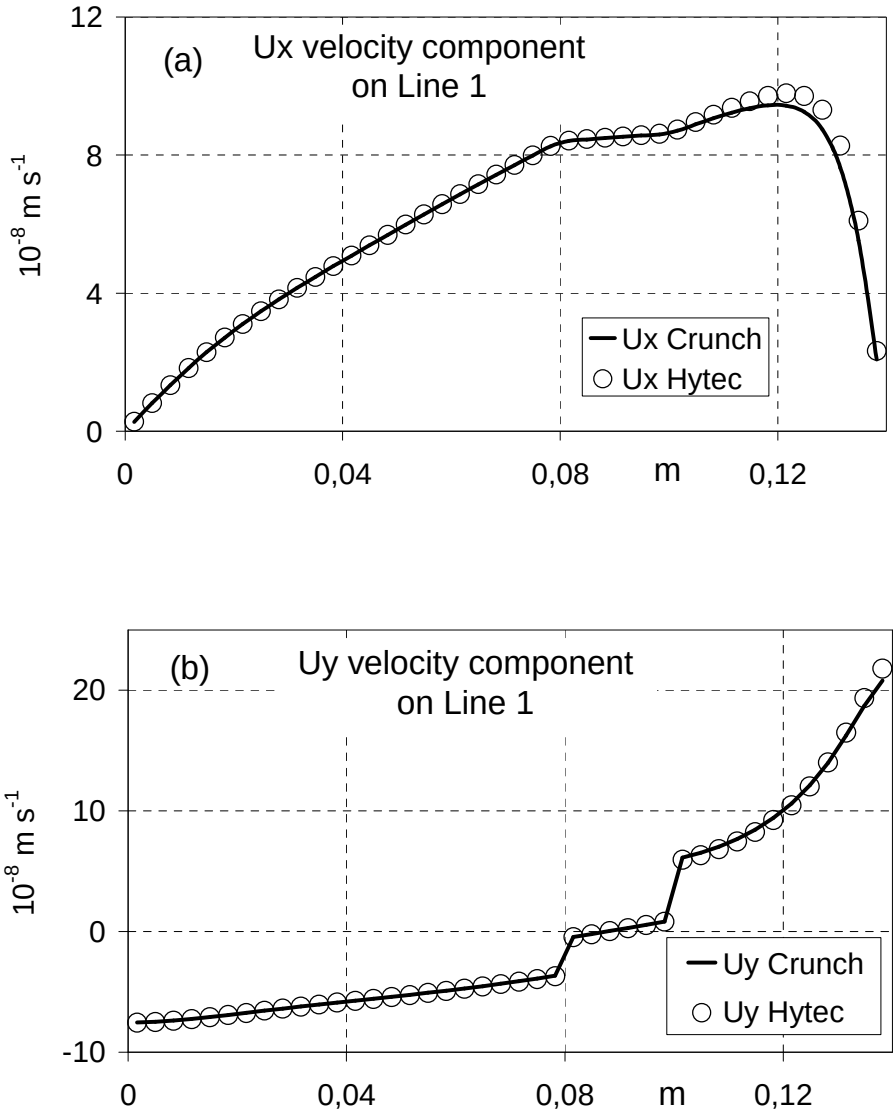
(a)
Ux velocity component
on Line 1
12
8
4
0
10^{-8} m s^{-1}
Ux Crunch
Ux Hytec
0
0,04
0,08
m
0,12
(b)
Uy velocity component
on Line 1
20
10
0
-10
10^{-8} m s^{-1}
Uy Crunch
Uy Hytec
0
0,04
0,08
m
0,12

Figure 2

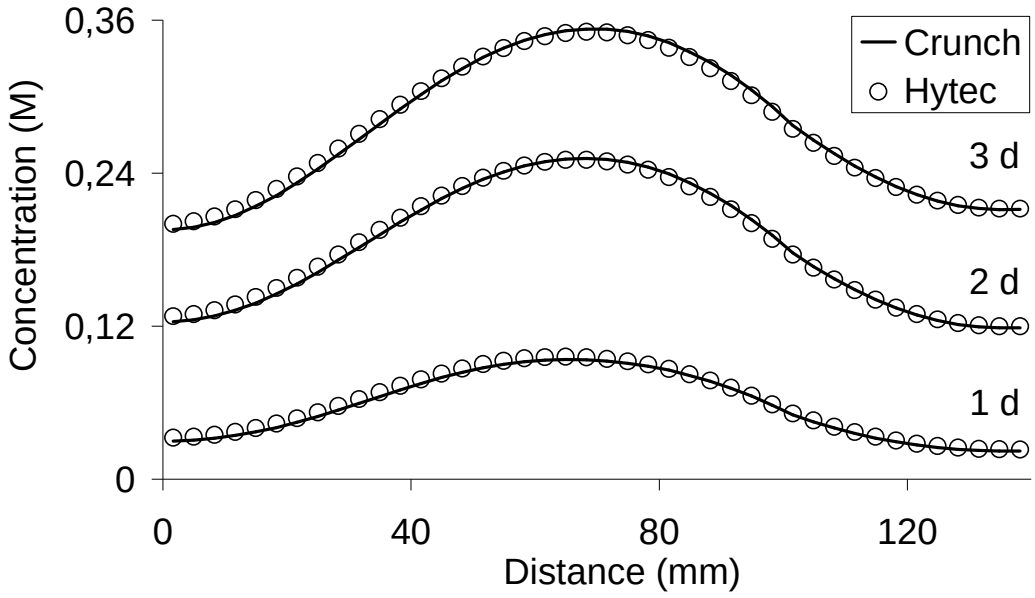
0,36
0,24
0,12
0
Concentration (M)
0
40
80
120
Distance (mm)
Crunch
Hytec
3 d
2 d
1 d

Figure 3

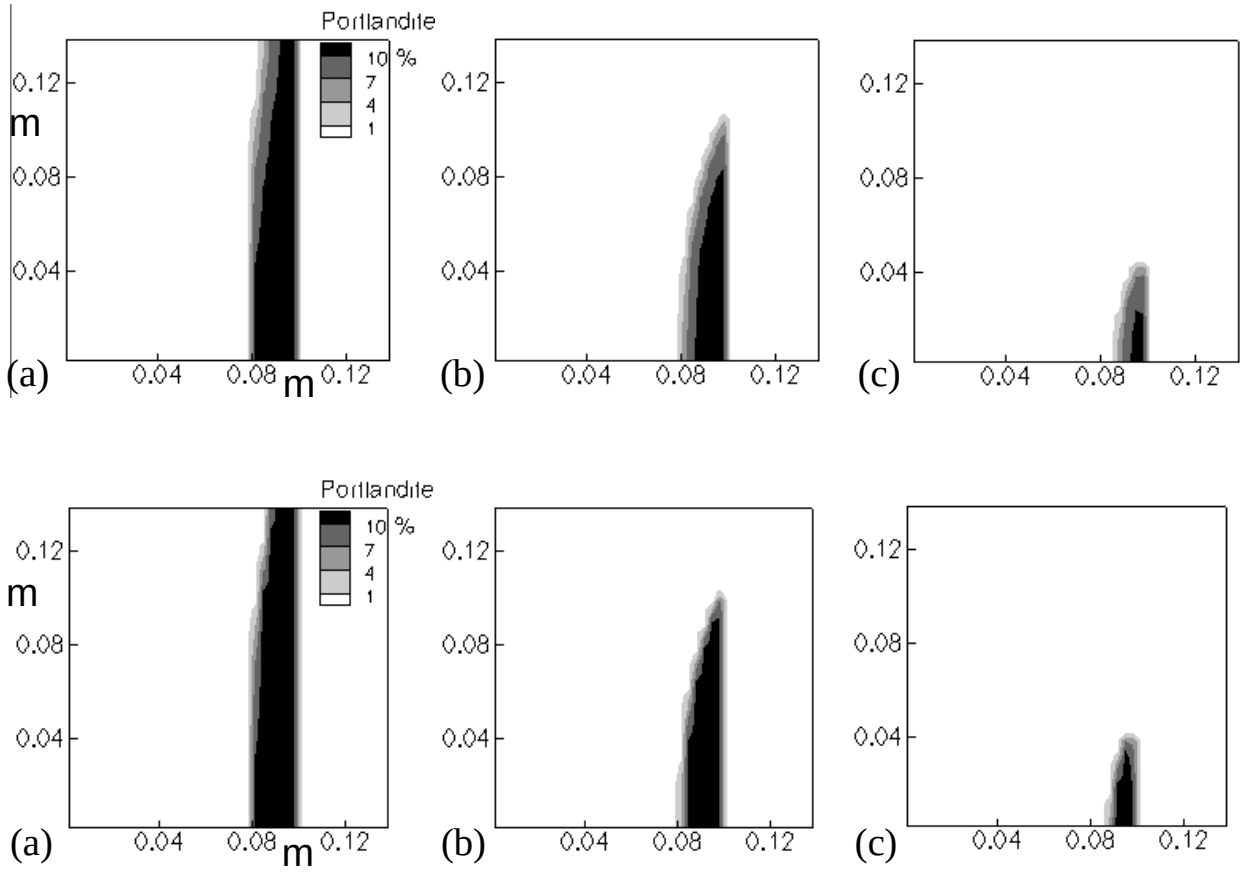
Portlandite
10 %
7
4
1
0.12
0.08
0.04
m
(a)
(b)
(c)
0.04
0.08
0.12
Portlandite
10 %
7
4
1
0.12
0.08
0.04
m
(a)
(b)
(c)
0.04
0.08
0.12
m

Figure 4

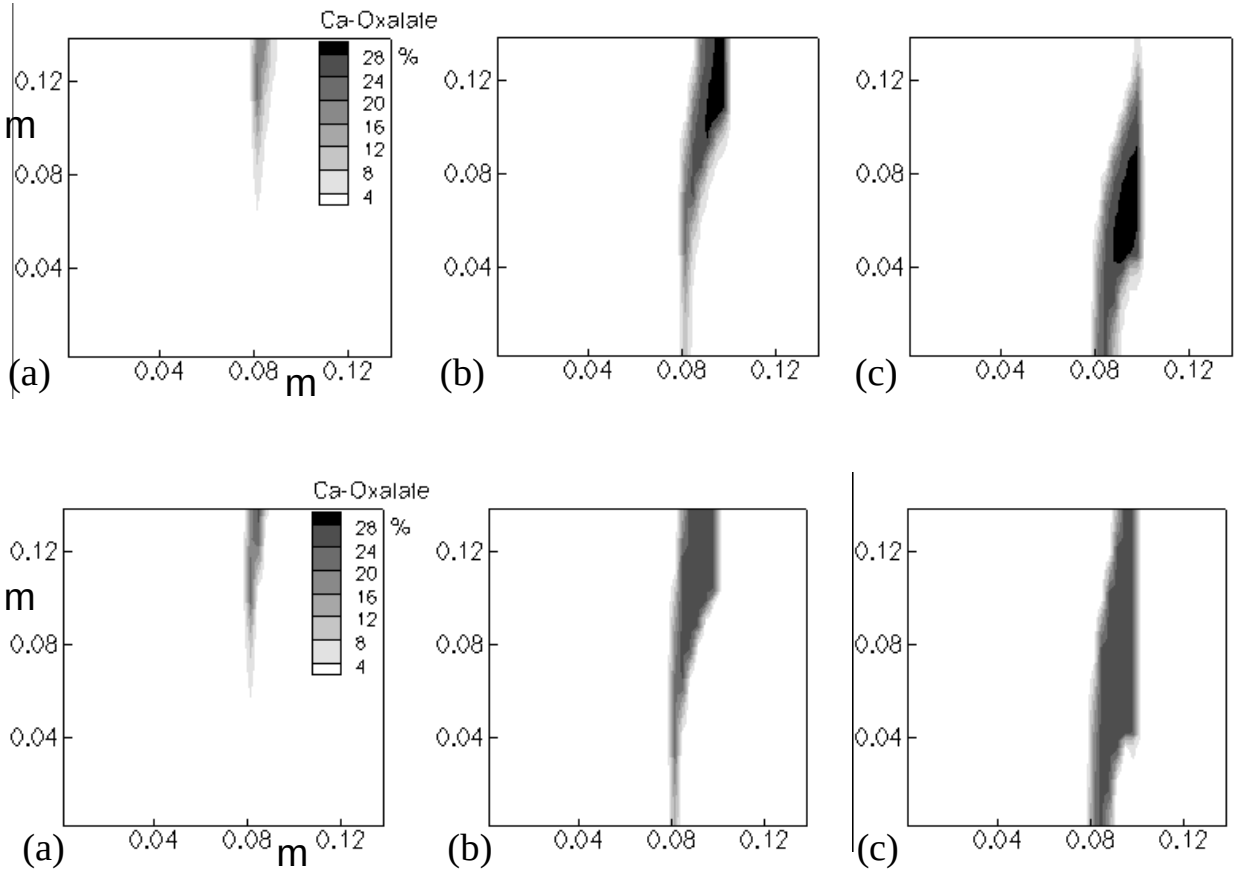

Figure 5

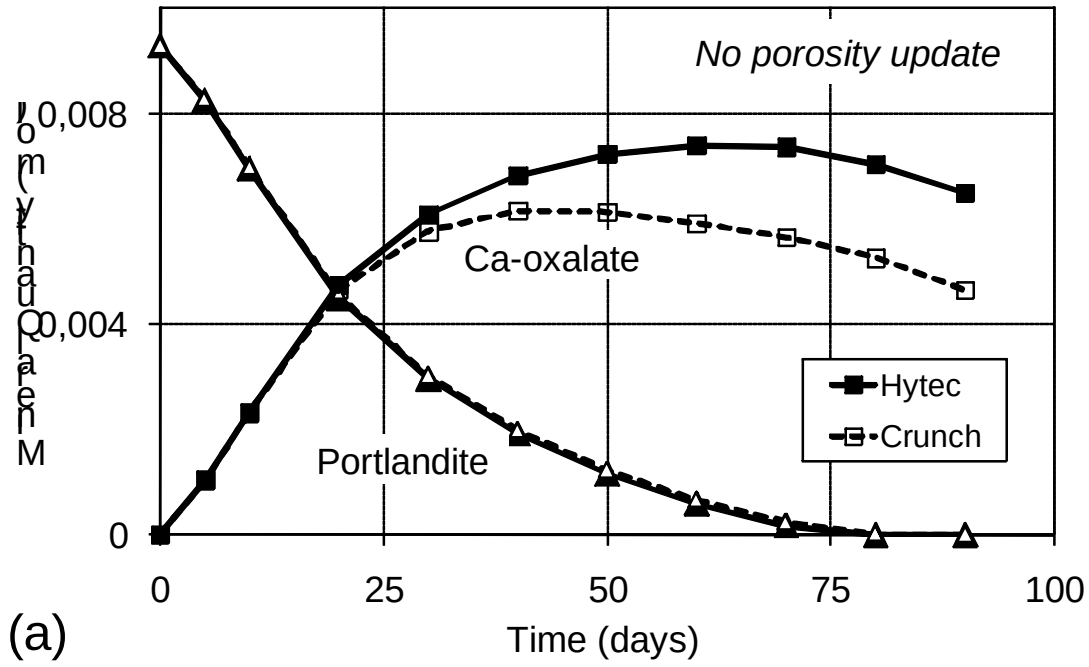
No porosity update
0,008
0,004
0
Ca-oxalate
Portlandite
Hytec
Crunch
0
25
50
75
100
Time (days)
(a)

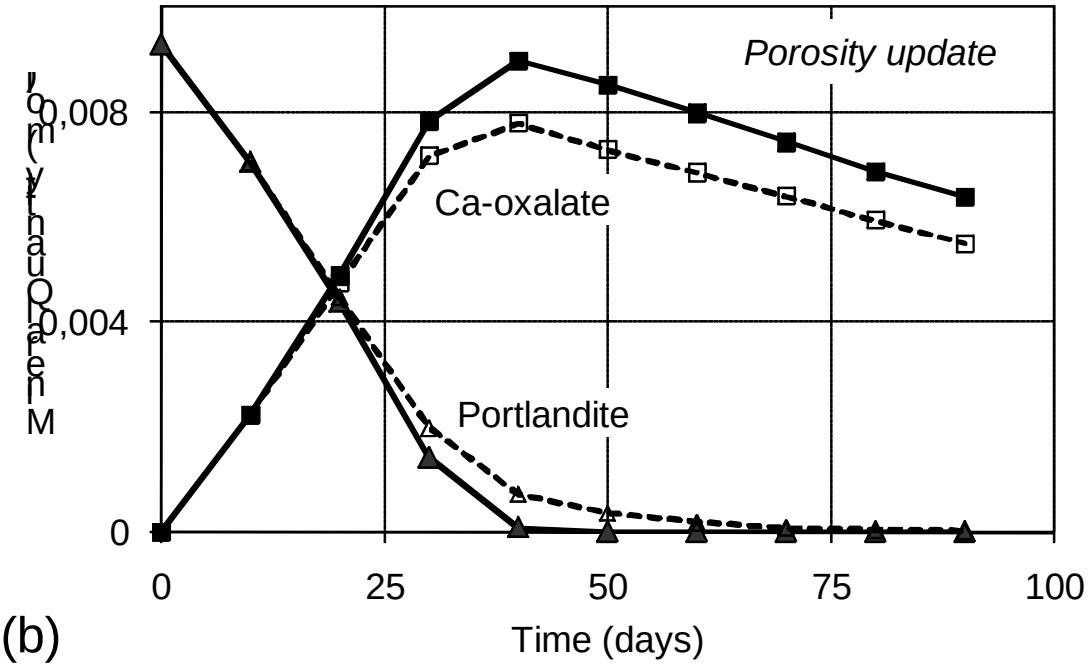
Porosity update
0,008
0,004
0
Ca-oxalate
Portlandite
0
25
50
75
100
Time (days)
(b)

Figure 6

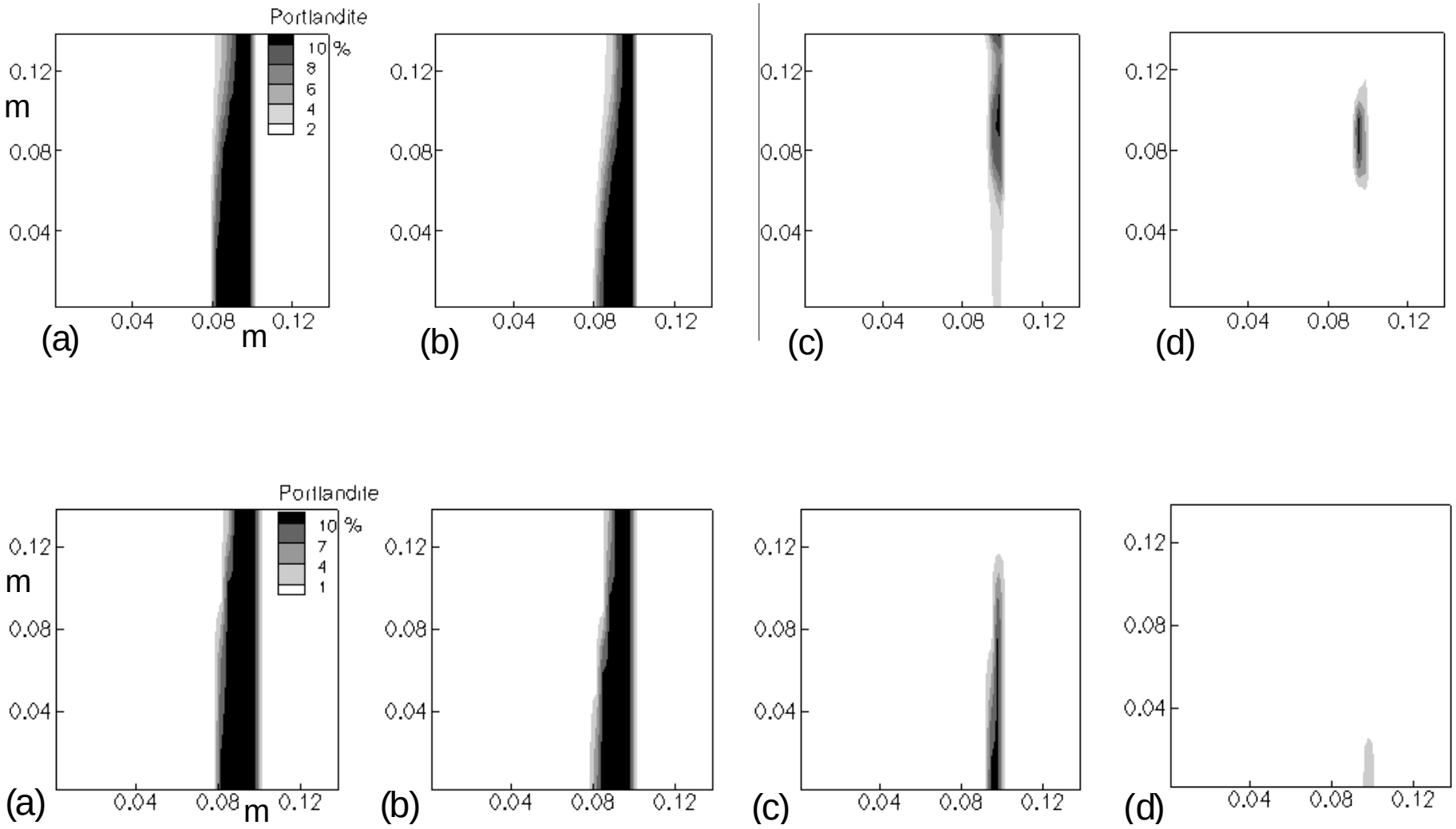
Portlandite
10 %
8
6
4
2
0.12
0.08
0.04
m
0.04
0.08
0.12
(a)
(b)
(c)
(d)
Portlandite
10 %
7
4
1

Figure 7

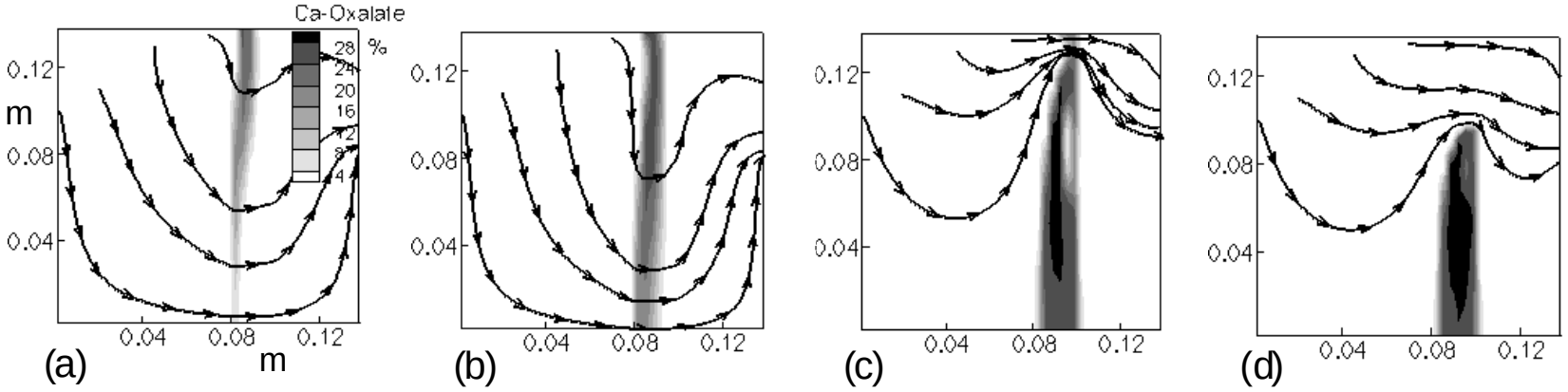

Figure 8

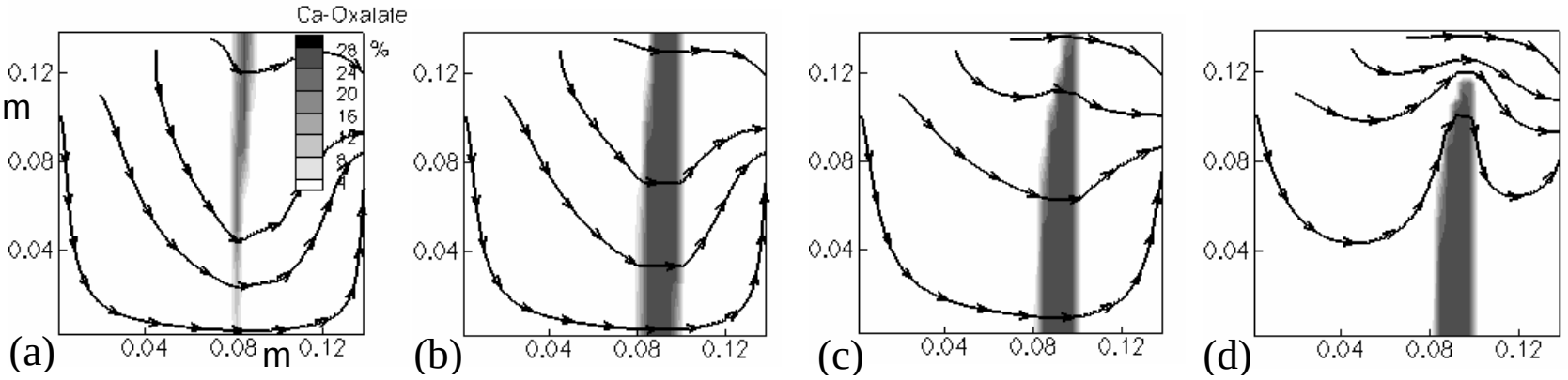

Figure 9

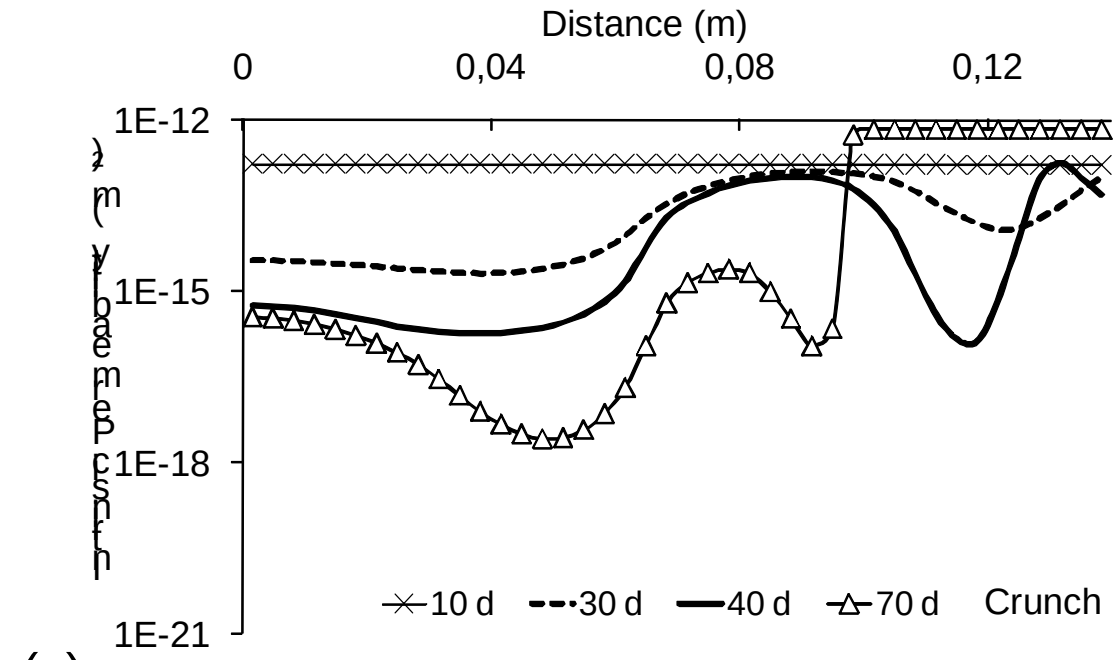
Distance (m)
0
0,04
0,08
0,12
1E-12
1E-15
1E-18
1E-21
10 d
30 d
40 d
70 d
Crunch

(a)

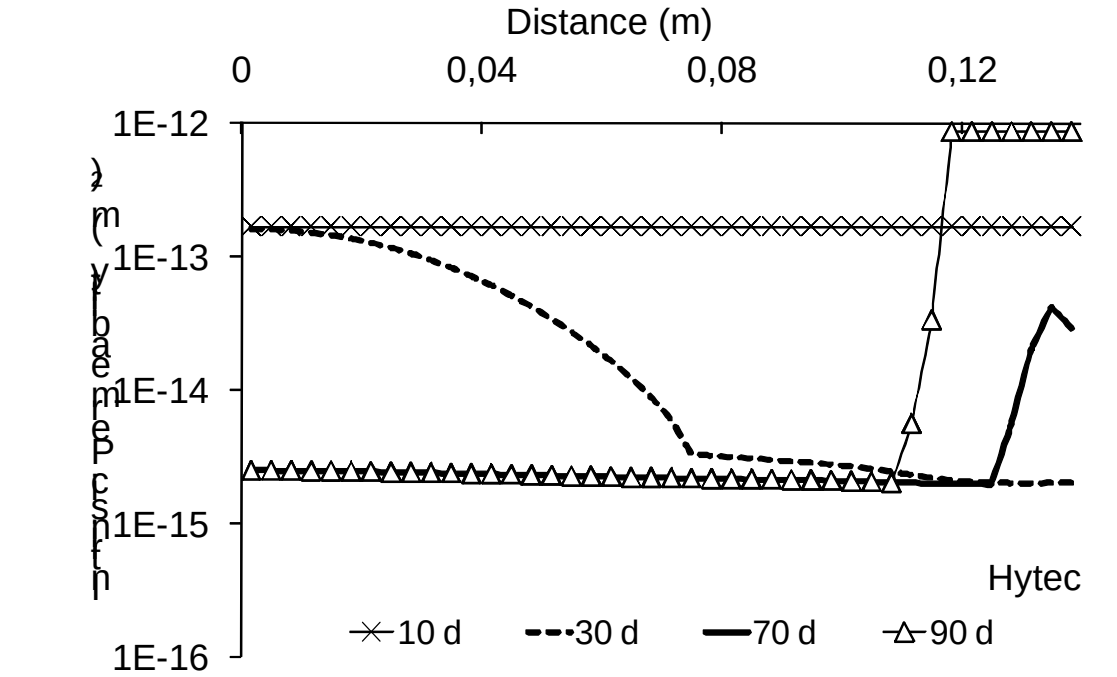
Distance (m)
0
0,04
0,08
0,12
1E-12
1E-13
1E-14
1E-15
1E-16
Hytec
10 d
30 d
70 d
90 d

(b)

Figure 10

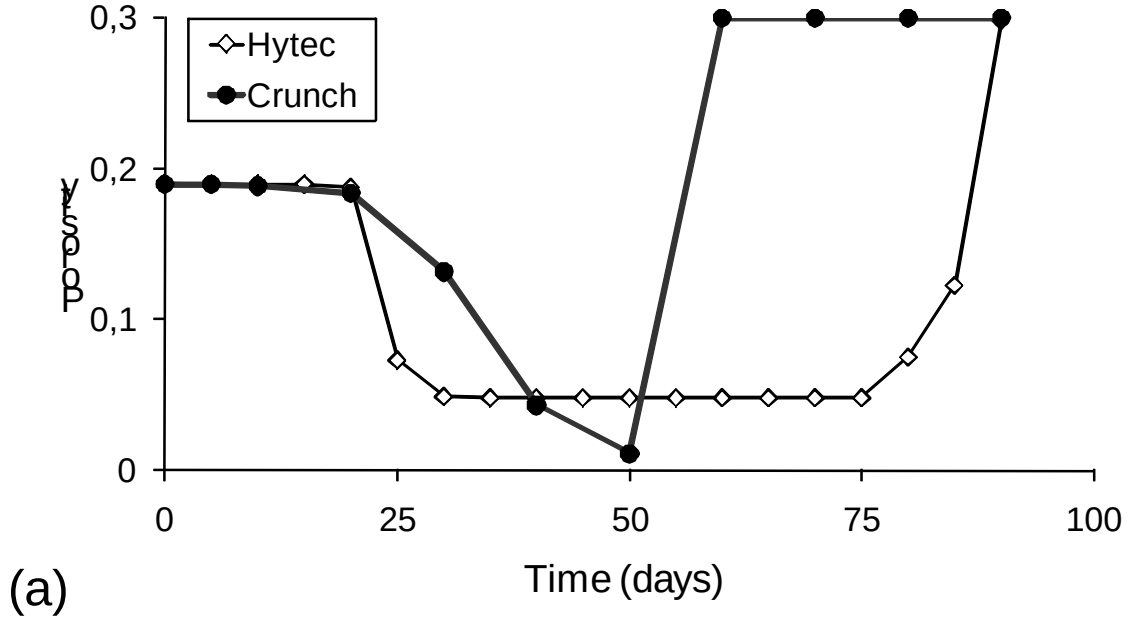
0,3
0,2
0,1
0
Hytec
Crunch
0
25
50
75
100
Time (days)

(a)

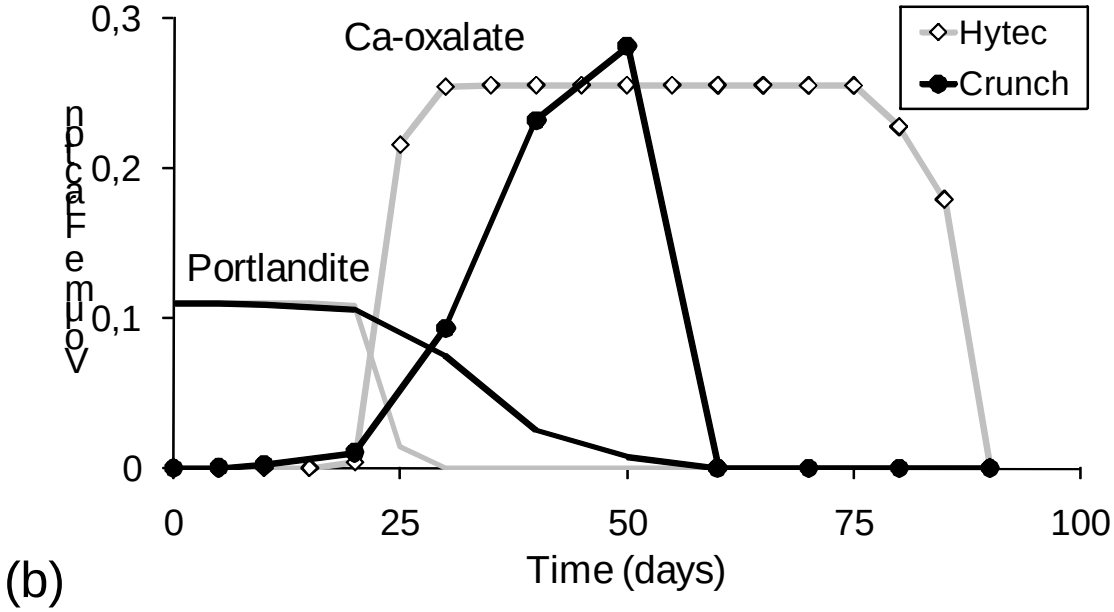
0,3
0,2
0,1
0
Ca-oxalate
Portlandite
Hytec
Crunch
0
25
50
75
100
Time (days)

(b)

Figure 11

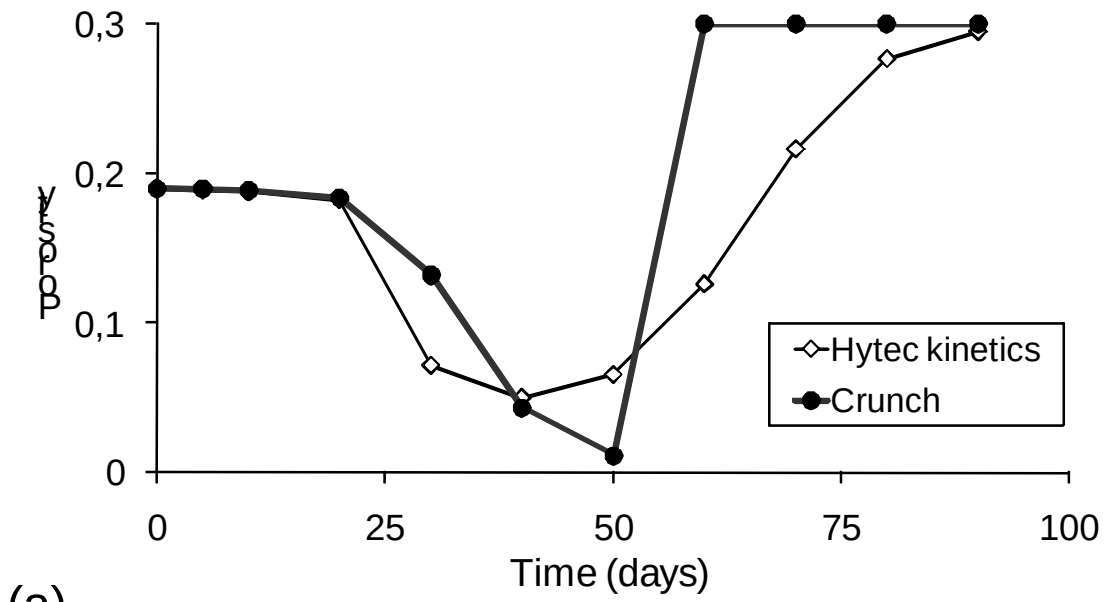
0,3
0,2
0,1
0
0
25
50
75
100
Time (days)
Hytec kinetics
Crunch

(a)

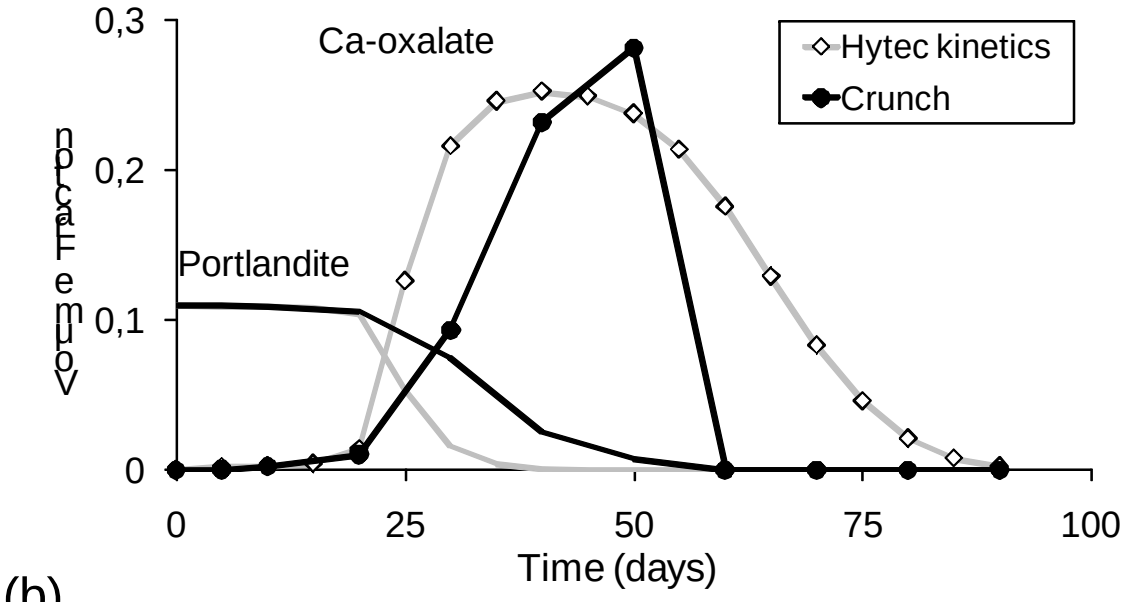
0,3
0,2
0,1
0
0
25
50
75
100
Time (days)
Ca-oxalate
Portlandite
Hytec kinetics
Crunch

(b)

Figure 12